

ZnO/Bone-Char Hybrid Composite: Catalyst Preparation, Characterization, and Its Application

**Damodhar, Ghime; Vijendra, Kumar; Titikshya, Mohapatra;
Neelam, Sonwani; Saket, Pradhan; Prabir, Ghosh*⁺**

Department of Chemical Engineering, National Institute of Technology, Raipur (CG), INDIA

Sandeep, Dharmadhikari

Department of Chemical Engineering, Guru Ghasidas Vishwavidyalaya, Bilaspur (CG), INDIA

Sudip, Banerjee

Department of Chemical Engineering, Indira Gandhi Institute of Technology Sarang, Dhenkanal, Odisha, INDIA

ABSTRACT: *This study was aimed at the development of the ZnO/bone-char (ZnO/BC) hybrid composite and it was characterized by its suitability for the treatment of dye-containing wastewater. The Zn/BC composites were prepared using four different methods such as sol-gel, precipitation, hydrothermal and wet-impregnation methods. Various analyzing techniques such as X-Ray Diffraction (XRD), Fourier Transform Infra-Red (FT-IR), Brunauer-Emmett-Teller (BET) surface area, and Scanning Electron Microscopy (SEM) were performed to characterize the prepared photocatalysts. The photocatalytic activity of the ZnO/BC composite prepared from the sol-gel method was evaluated by the decolorization of brilliant green dye in an aqueous solution. The results of SEM analysis confirm the agglomeration of nano-ZnO particles and particles are evenly distributed on the surface of the bone char. Moreover, the influence of different experimental parameters like solution pH, H₂O₂ concentration, and photocatalyst dosage was studied to optimize the process efficiency. This study also shows that chicken bone waste can be used as a photocatalyst carrier for the synthesis of photocatalytic composites. It not only provides a better way to treat dye-containing wastewater but also offers an ideal solution to using chicken bone waste. From the kinetic analysis, it has been observed that the photocatalytic decolorization of BG dye with ZnO/BC photocatalyst follows pseudo-first-order kinetics.*

KEYWORDS: *Development of catalyst; Photocatalytic activity; Brilliant green dye; Environmental pollution; Wastewater treatment; Kinetics.*

INTRODUCTION

Water pollution is a global environmental issue among environmental pollutions. Industrialization and an increase in population density led to producing

a large volume of wastewater, which contains a variety of refractory organic pollutants. The dye is a significant water contaminant, which has drawn the attention of

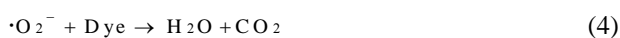
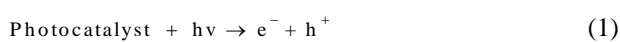
**To whom correspondence should be addressed.*

+E-mail: prabirg.che@nitrr.ac.in

1021-9986/2022/4/1186-1198

14/\$/6.04

environmental researchers, because it is generally found in the released effluents of several industries like textile, paper and pulp, tannery, food processing, etc. According to the estimated amount, approximately 100,000 types of synthetic dyes are produced annually, and 10% of total dye production is released into the environment. Being a toxic compound, it has some adverse effects on both the aquatic biota and human beings [1]. Therefore, it is needed for proper treatment before its discharge into freshwater bodies. Since the dye has complexity in its structure, it shows resistance to biological degradation [2]. Nowadays, heterogeneous photocatalysis is a rising technique for the remediation of water contaminants. Zinc oxide (ZnO) and Titanium dioxide (TiO₂) are commonly used semiconductors for photocatalysis processes. However, in recent years, ZnO is a broadly used photocatalyst compared to TiO₂, as it can absorb a significant fraction of the UV spectrum [3, 4]. It also has high thermal conductivity, a wide range of bandgap (3.37 eV), and is low in cost. When ZnO is illuminated under sufficient lighting conditions, it generates electron/hole pairs (e⁻/h⁺), as shown in Eq. (1). These electron/hole pairs further react with the water (H₂O) molecules along with the dissolved oxygen (O₂) in the water and generate hydroxyl radicals (HO•) and superoxide radicals (•O₂⁻), represented in Eqs. (2, 3) [5]. These produced radicals non-selectively react with the dye molecule in wastewater and break them into simpler compounds as per Eq. (4) and Eq. (5)[6].



It has been reported that combining metal ions with carbon material develops photocatalytic activity and helps to achieve complete mineralization of the water pollutant. There are various carbon materials like activated carbon, graphene, graphite, carbon nanotube, and bone char. But, among them, Bone Char (BC) is preferable due to its porous structure, various surface functional group, sustainability, and cost-effectiveness [7]. Moreover, the bone char is composed of main

hydroxyapatite with a large surface area for the reaction to happen. It shows the significant adsorption for various types of textile dyes. In order to meet the regular dietary requirement, a large number of animals are used, and subsequently, it generates bone as a by-product. Handling these bones at the right time is very important, otherwise, it turns into solid waste, breed bacteria, jeopardizes the health of human beings, also pollute the environment [8]. So, the conversion of these bones into bone char not only controls solid waste but also helps in the treatment of environmental pollution. Bone-char is having certain advantages, such as alkali resistance, good adsorption ability, thermostability, water insolubility, non-toxicity, and recyclability. This makes the bone char an effective candidate for making the composites with ZnO. Reported researches show that Zn embedded in bone char prepared from bovine bone can be used for the photo-degradation of various organic contaminants and significant degradation efficiency was achieved [4, 8, 9]. *Jia et al.* (2018) used ZnO/BC composite prepared by a simple precipitation method to degrade methylene blue dye [4]. It has been observed that the immobilization of ZnO on a large-sized bone char has a synergetic effect on the photocatalytic degradation of water pollutants. Thus, the combination of both ZnO and bone-char form an effective composite for the remediation of dyes in industrial wastewater. *Rezaee et al.* (2014) decomposed formaldehyde by using Bone-Char (BC) immobilized with nano-ZnO particles. But through the physical mixing, the nano-sized ZnO particles are unable to evenly disperse onto the bone-char surface [15]. To achieve better catalytic activity, the layer of ZnO nanoparticles should be uniformly loaded on the surface of bone char. This green degradation technology uses photo-catalytic oxidation for the removal of toxic pollutants in industrial effluent. It also helps in solving serious environmental issues. Therefore, the present work focuses on the synthesis of Bone Char (BC) supported zinc oxide (ZnO/BC) composite via four different methods such as sol-gel, precipitation, hydrothermal and wet-impregnation methods. The prepared photocatalyst was further characterized by X-Ray Diffraction (XRD), Fourier Transform Infra-Red (FT-IR), Brunauer-Emmett-Teller (BET) surface area, and Scanning Electron Microscopy (SEM) analyses. The decolorization of dye-containing wastewater has been successfully investigated through the photocatalytic activity of sol-gel mediated photocatalyst.

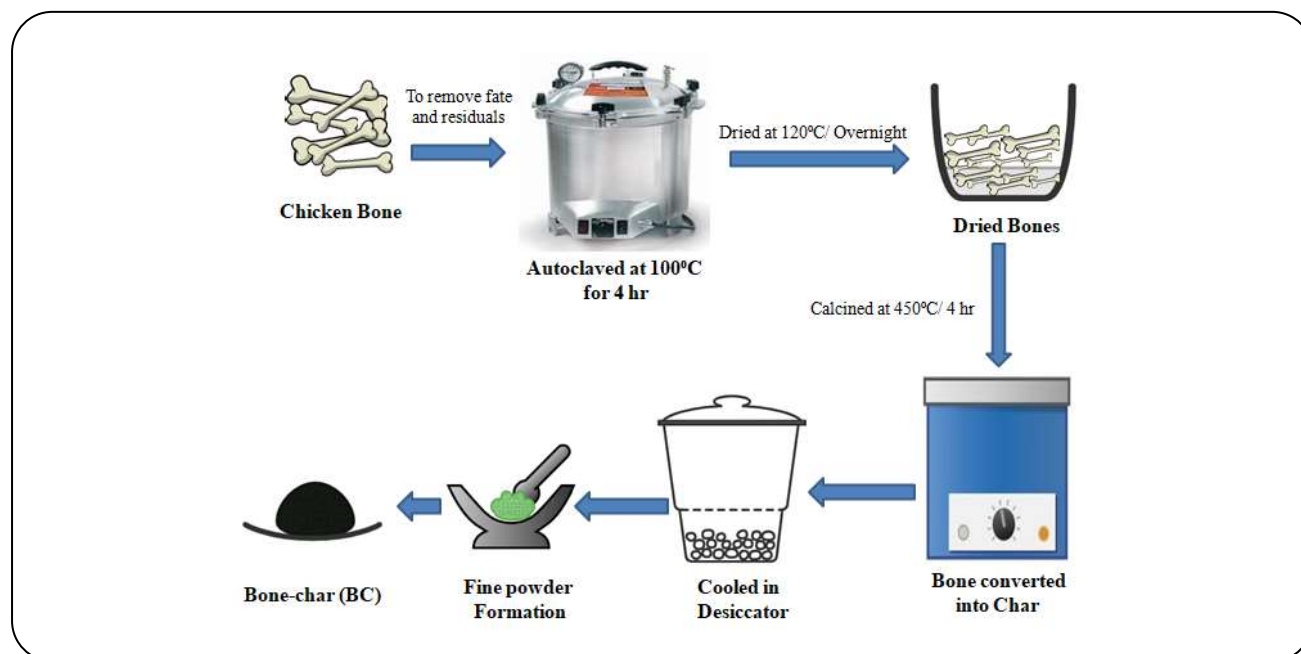


Fig. 1: Flow diagram for the preparation of bone char.

The brilliant green dye was chosen as a model pollutant. Brilliant Green (BG) is a cationic dye and is widely used in the paper and textile industries. Mostly, it has been used in the dyeing of wool and silk materials. Around 0.8-1 kg of BG dye is required per ton of paper production. This dye is hazardous to skin, eye contact, and ingestion. Through inhalation, it can affect the lungs and frequent exposure can damage the target organ [10, 11]. The influence of different experimental parameters such as solution pH, the effect of H_2O_2 concentration, and photocatalyst dosage was studied for the treatment of wastewater containing brilliant green dye.

EXPERIMENTAL SECTION

Materials

Chicken bone waste was collected from the local mutton market in Raipur city, Chhattisgarh, India. Brilliant Green dye (90% purity) was procured from Sigma-Aldrich. Zinc sulphate (ZnSO_4), sodium hydroxide (NaOH), ethyl alcohol ($\text{C}_2\text{H}_5\text{OH}$), zinc oxide (ZnO), and oxalic acid ($\text{C}_2\text{O}_4\text{H}_4$, 12.6 g) were purchased from Merck. All the chemicals used for the photocatalyst preparation and in experimental runs were of analytical grade.

Preparation of Bone Char (BC)

2kg of chicken bone waste was taken from the market and rinsed three times with deionized water. Subsequently,

it was kept in an autoclave at 100°C for 4 h. The bones were dried at 120°C in a hot air oven and further cooled in the desiccators. Finally, the dried bones were calcined at 450°C for 4 h, resulting in the formation of BC. This was then crushed in a pestle mortar and stored for further use [9]. Fig. 1 shows the flow diagram for the preparation of bone char.

Synthesis of ZnO/BC photocatalyst with the different methods

Wet impregnation method

An aqueous solution of ZnSO_4 was prepared. 10g of bone char was added to the prepared solution, mixed, and stirred in a magnetic stirrer at 570 rpm to get a homogenous mixture. The obtained precursor solution was dried at 105°C for 12 h. Finally, the product was calcined at 500°C for 4 h to get ZnO/BC photocatalyst [12].

Hydrothermal method

An aqueous solution of sodium hydroxide (NaOH) and H_2O was prepared in a ratio of 1:1. Then, 10g of bone char and 3.4g of ZnSO_4 were mixed with it. For homogenous mixing, the mixture was stirred for 10 min at 570rpm. Subsequently, the homogenous mixture was transferred to the Teflon-lined autoclave and heated in the oven at 180°C for 2 h. The solution was allowed to cool down completely and then the resultant was filtered, followed by washing with deionized water and ethanol

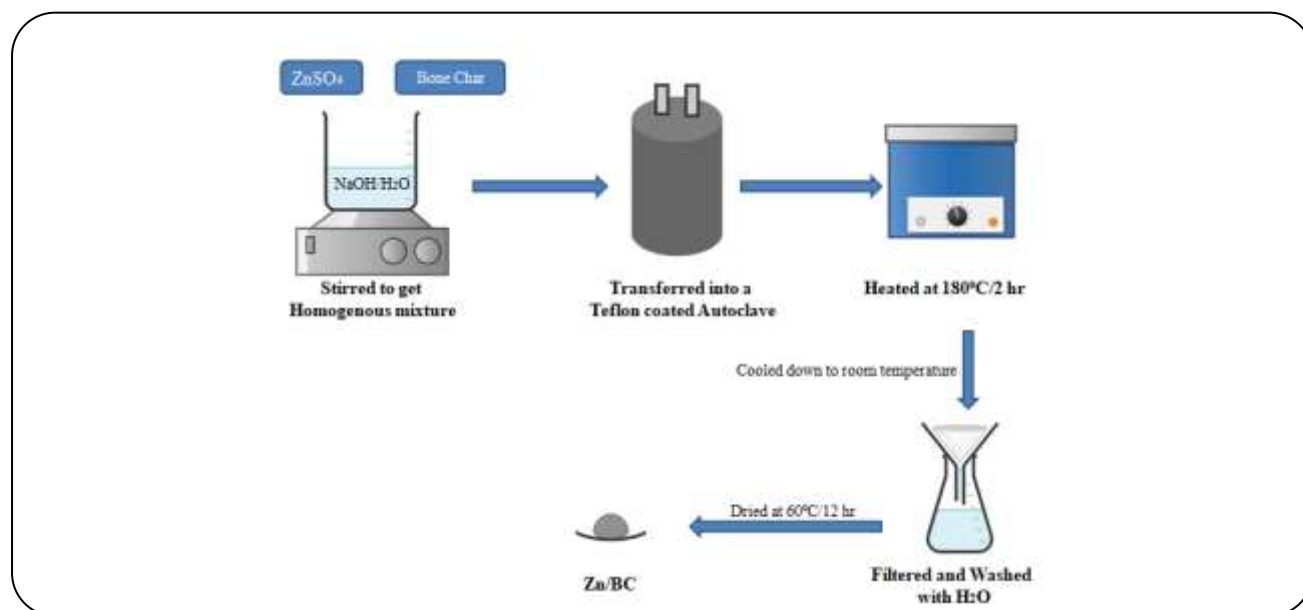


Fig. 2: Flow diagram for the preparation of ZnO/BC photocatalyst by hydrothermal method.

to remove any impurities present in it. The filtered solution was dried at 60°C in the hot air oven for 12 h to get the ZnO/BC photocatalyst [13]. Fig. 2 shows the flow diagram for the preparation of Zn/BC by the hydrothermal method.

Precipitation method

Zn precursor was prepared by adding 3.4 g of $ZnSO_4$ in a mixture of water and ethanol in 1:1 ratio. Subsequently, 10 g of bone char was added to this solution and stirred to get a homogenous mixture. Sodium hydroxide was used as a reducing agent, and the dropwise addition of NaOH solution into the homogenous mixture resulted in precipitated formation. The precipitate was filtrated out and dried at 110°C for 4 h in a hot air oven [14]. Then, the dried sample was calcined at 400°C for 4 h in a muffle furnace to obtain ZnO/BC photocatalyst. Fig. 3 shows the flow diagram for the synthesis of Zn/bone char by precipitation method.

Sol-gel method

The preparation of Zn/BC photocatalyst by the sol-gel method is a two-step procedure. In the first step, a solution was prepared by adding zinc acetate to ethanol at 60°C. Separately, the oxalic acid solution was also prepared by adding it to ethanol at 50°C. This prepared solution was slowly added to the zinc acetate solution under constant stirring, resulting in the formation of a thick white gel.

Then, the thick white gel was dried in the oven and the dried product was further calcined at 500°C for 2 h to get Zn nanoparticles. In the second step, Zn nanoparticles and 10 g of bone char were added into an aqueous solution and stirred continuously for 3 h. Afterward, the homogenous mixture was filtered and at room temperature, it was dried, followed by calcination at 300°C for 2 h to obtain Zn/BC photocatalyst [15]. Fig. 4 shows the flow diagram for the synthesis of Zn/bone char by the sol-gel method.

Characterization of the fabricated photocatalysts

The synthesized Zn/BC photocatalysts from different processes were characterized by X-Ray powder Diffraction (XRD) to obtain the structure of the catalyst. To evaluate the morphology, the samples were characterized by Scanning Electron Microscopy (SEM, model: ZEISS EVO 18 series). Fourier Transform Infrared spectroscopy (FTIR) was performed by Bruker, Alpha-model to know about the functional groups present on the catalyst surface. Also, the photocatalysts were characterized by a BET surface area analyzer (Smart instruments, India, and single point) for the surface area, pore volume, and average diameters.

Experimental Procedure

The experimental runs for the decolorization of brilliant green dye were carried out in a cylindrical

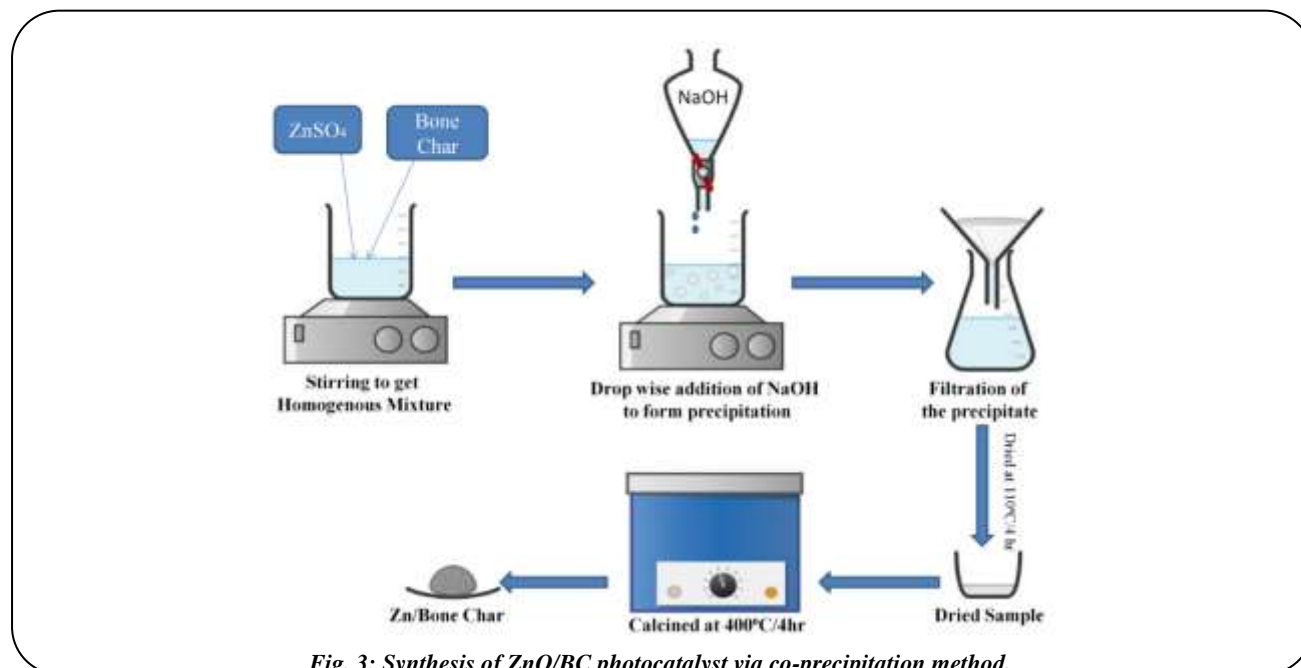


Fig. 3: Synthesis of ZnO/BC photocatalyst via co-precipitation method.

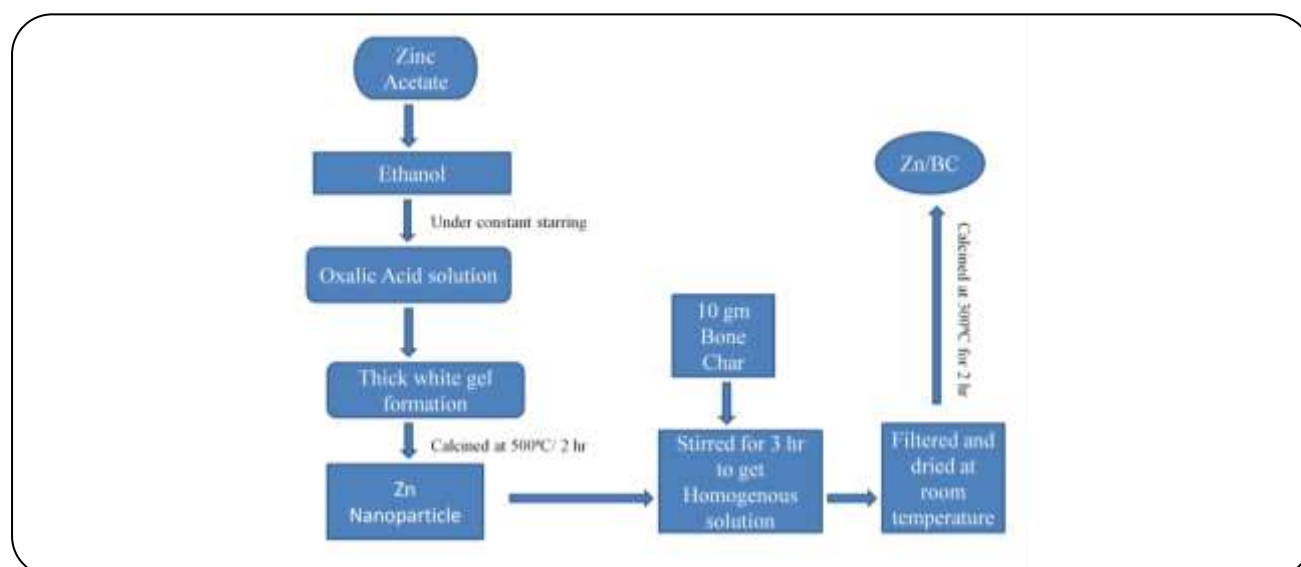


Fig. 4: Preparation of ZnO/BC photocatalyst by the sol-gel method.

photochemical reactor having a maximum capacity of 300 mL, which was internally installed with a 125W UV lamp. A magnetic stirrer was also provided with the reactor to mix the dye solution properly. Initially, the photocatalyst was added to the photochemical reactor. There are two ports supplied on either side of the reactor, through which 250 mL of 100 ppm BG dye solution was inserted into the glass/quartz build feed tank. Then the reactor and its stirrer were switched on. The dye solution keeps on mixing in the reactor, exposed to the UV light in addition

to the catalyst dose with oxidant (H₂O₂), and thus, a photocatalytic reaction occurs. The samples were collected after a specific time interval and analyzed through absorbance value obtained by a UV-Visible Spectrophotometer (model: UV 1800 Shimadzu). The equation obtained for the calibration curve of the BG dye solution was $Y=0.0705X+0.0381$, $R^2=0.9717$; where Y is the absorbance value for brilliant green dye at 625 nm and X is the BG dye concentration. The decolorization percentage of BG dye was evaluated by Eq. (6).

$$\text{Decolorization percentage of BG (\%)} = \frac{C_i - C_t}{C_i} \times 100 \quad (6)$$

Where C_i = initial concentration of BG dye and C_t = BG dye concentration at time t .

RESULTS AND DISCUSSION

Characterization of prepared catalysts

X-Ray powder Diffraction (XRD) analysis of ZnO/BC photocatalyst

XRD analysis is a technique used for determining the atomic and molecular structure of a crystal, in which the crystalline structure causes a beam of incident X-rays to diffract into many specific directions. By measuring the angles and intensities of these diffracted beams, a crystallographer can produce a three-dimensional picture of the density of electrons within the crystal. From this electron density, the mean positions of the atoms in the crystal can be determined, as well as their chemical bonds, their crystallographic disorder, and various other information [16].

From Fig.5(a), it was observed that the prepared sample was crystalline in nature. The diffraction peaks appeared at 2θ equal to $31.693^\circ, 33.115^\circ, 46.945^\circ, 47.005^\circ$ correspond to hexagonal crystal lattices (200), (220), (104), (220) with diffraction spacing $d(\text{\AA})$ of 2.821, 1.933, 2.703, 1.931, respectively. This shows the presence of sodium chloride (NaCl), copper iron sulphide (Cu_5FeS_4), iron oxide (Fe_2O_3), and calcium fluoride (CaF_2) [16]. From Fig.5(b), the diffraction peaks appeared at 2θ equal to $31.693^\circ, 66.115^\circ, 46.945^\circ, 47.005^\circ$ correspond to the hexagonal crystal lattices (200), (104), (220), (220) with $d(\text{\AA})$ spacing 2.821, 2.703, 1.933, 1.931, respectively. This shows the presence of sodium chloride (NaCl), iron oxide (Fe_2O_3), copper iron sulphide (Cu_5FeS_4), and calcium fluoride (CaF_2). Fig.5(c) shows that the diffraction peaks appeared at 2θ equal to $44.393^\circ, 47.005^\circ, 33.115^\circ, 46.945^\circ$ correspond to the hexagonal crystal lattices (110), (220), (104), (220) with $d(\text{\AA})$ spacing of 2.039, 1.931, 2.703, 1.923 respectively. This shows the presence of chromium (Cr), calcium fluoride (CaF_2), iron oxide (Fe_2O_3), and copper iron sulphide (Cu_5FeS_4). Fig.5(d) represents that the diffraction peaks that appeared at 2θ equal to $31.693^\circ, 29.406^\circ, 28.261^\circ, 28.443^\circ$ correspond to the hexagonal crystal

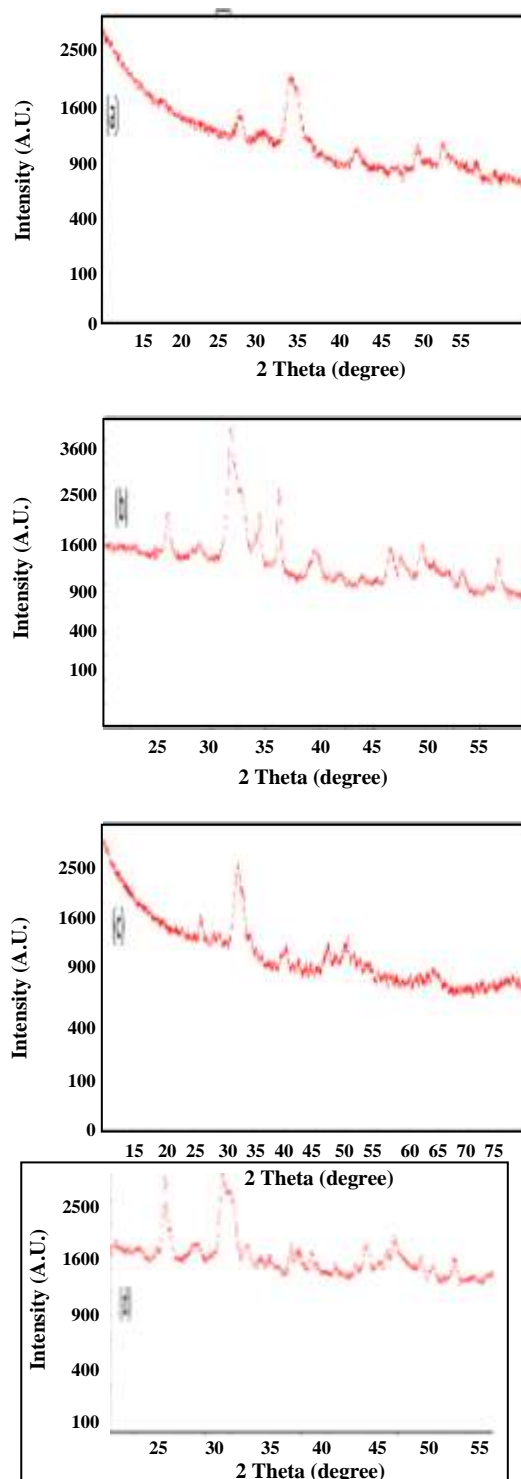
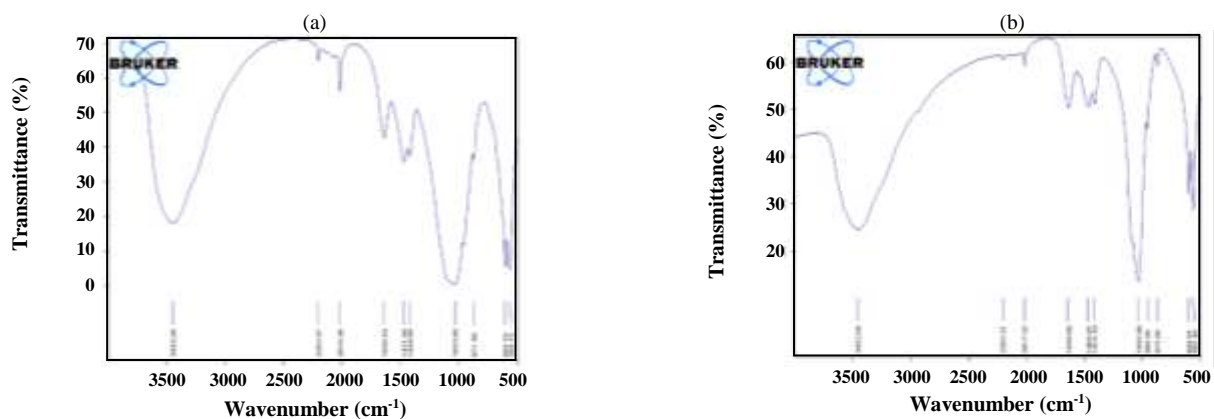
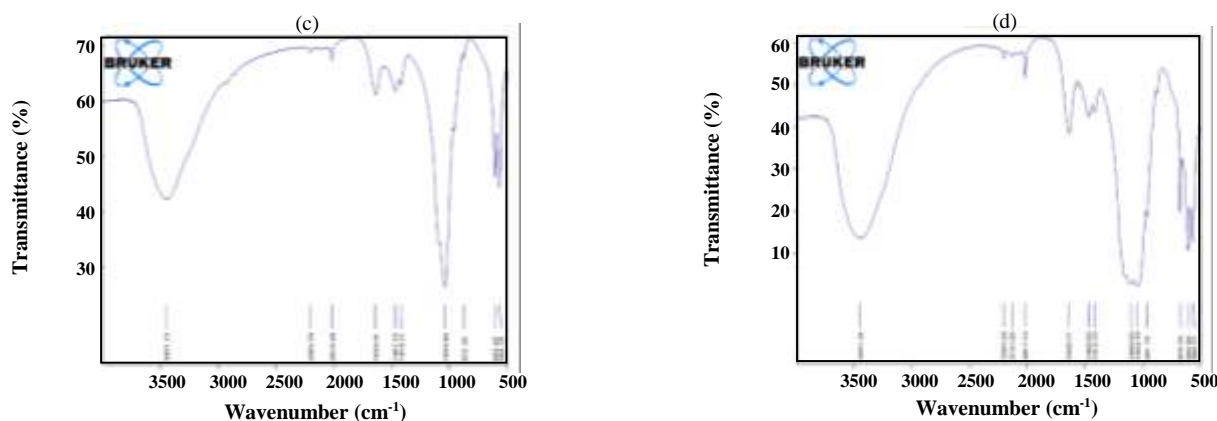


Fig. 5: XRD plot of photocatalyst prepared by (a) wet impregnation method (b) hydrothermal method (c) sol-gel method and (d) co-precipitation method.

Table 1: FTIR results of ZnO/BC photocatalyst with the different peaks associated with it.

Associated peaks	Group Characterization	References
3445-3452 cm^{-1}	stretching of hydroxyl ($-\text{OH}$)	[18, 19]
1600-1650 cm^{-1}	stretching of hydroxyl ($-\text{OH}$)	[18, 19]
872 cm^{-1}	Out-of-plane bending in CO_3^{2-}	[20]

**Fig. 6: FTIR plot of catalyst prepared using (a) wet impregnation method (b) hydrothermal method.****Fig. 7: FTIR plot of catalyst prepared using (c) sol-gel method and (d) co-precipitation method.**

lattices (200),(104),(111),(111) with $d(\text{Å})$ spacing 2.821,3.035,3.155,3.135, respectively. This shows the presence of sodium chloride (NaCl), calcium carbonate (CaCO_3), sodium erbium fluoride (NaErF_4) and silicon (Si) [17].

Fourier Transform Infrared spectroscopy (FT-IR) of ZnO/BC photocatalyst

The prepared photocatalyst was characterized by FT-IR using Bruker, Alpha model in a wide range 3500-500

cm^{-1} that gives the information about the functional groups present on the catalyst surface along with intra and intermolecular interaction. Similar peak values were observed in all the graphs shown in Fig. 6 and Fig. 7. The broadband at 3445-3452 cm^{-1} and a band at 1600-1650 cm^{-1} is due to the stretching of hydroxyl ($-\text{OH}$) functional groups, that resulted from the moisture content on the catalyst surface [18, 19]. While the bands at 1415-1471 cm^{-1} , 872 cm^{-1} are attributed to the carbonate bands, which is possible because of the adsorption of atmospheric CO_2

Table 2: BET analysis results of ZnO/BC photocatalysts.

Method	Pore Volume(cc/g)	Surface Area(m ² /g)	Average Pore Diameter (A ^o)
Wet impregnation	0.5441	35.061	620.746
Precipitation	0.0393	31.493	49.915
Hydrothermal	0.154	60.294	102.166
Sol-Gel	0.1601	61.034	104.925

at the time of catalyst synthesis [20]. The bands at 564, 603, 604, 605, 960, 961, 1033, 1034, 1035, 1044, 1099 cm⁻¹ are the characteristic of phosphate structure (PO₄³⁻) [21]. Table 1 shows the FT-IR results of ZnO/BC photocatalyst with the different peaks associated with it.

Brunauer-Emmett-Teller (BET) analysis of ZnO/BC photocatalyst

The synthesized Zn/BC photocatalysts from different methods were characterized by BET, a single-point surface area analyzer. Table 2 shows the data for the surface area, pore volume, and average diameters of the modified photocatalysts. The higher surface area and a considerable proportion of low-coordinated surface atoms have been proven to extensively influence the physical and chemical properties of inorganic materials [4].

Scanning electron microscope (SEM) analysis of ZnO/BC photocatalysts

SEM analyzed the morphological study of the fabricated photocatalysts. Fig. 8 represents the SEM image obtained from prepared catalysts. It shows the aggregation of Zn particles on the surface of bone char. It was also confirmed that the single uniform layer of ZnO particles was distributed evenly on the surface of bone char [9, 22].

Effect of initial dye concentration on its decolorization efficiency

To observe the effect of initial dye concentration on the extent of brilliant green dye degradation, the dye concentration was varied in the range of 50 to 200 ppm under 125W UV-lamp irradiation. The rate of photolysis of dye depends on the scission of the sigma bond through which hydroxyl radical's formation happens [23]. Firstly, the dye molecule gets excited when one photon remains attached to it, subsequently, the excited molecules react with the free radicals to achieve the oxidation of the dye molecule in the effluent. As shown in Fig. 9, the

degradation efficiency increases with an increase in dye concentration from 50 to 100 ppm, it may be due to the more reactions between free radicals and dye molecules [14]. The dye removal for this decolorization study showed very high uptake removal of BG dye at its lower concentrations (50 to 100 ppm). The dye removal efficiency decreases with an increase in the initial dye concentrations (beyond 100 ppm). This might have happened due to the saturation of the sorption sites (free radicals) as the concentration of dye increases [24]. The actual amount of dye molecules adsorbed increases with the increase in its initial concentration. Thus, the increase in adsorption is limited by free radicals. This fact may be attributed to the phenomenon of the increase in the driving force of the concentration gradient, with the increase in the initial dye concentration. Therefore, the higher initial concentration of the dye element enhances the adsorption process. From the obtained results, it is clear that the further increase in dye concentration from 100 to 200 ppm resulted in a decrease in decolorization efficiency by 6.79%. Therefore, 100 ppm dye concentration was taken throughout the experimental runs.

Effect of pH on decolorization

The dye solution pH plays a vital role in the photodegradation process. The pH of different dye solutions varies to ensure strong adhesion of dye molecules to the objects to be colored. It is considered one of the factors, which governs the appropriate remediation process [25]. In the photo-catalysis processes, the decolorization of dye proceeds through different steps. The dye molecules diffuse from the bulk of the solution to the surface of the photocatalyst. When the whole system is irradiated with a suitable source of light having sufficient energy to activate the photocatalyst, decolorization begins. Once the possible dye decolorization occurs, the reaction products are desorbed from the photocatalyst surface and diffused back into the bulk of the solution. The pH is

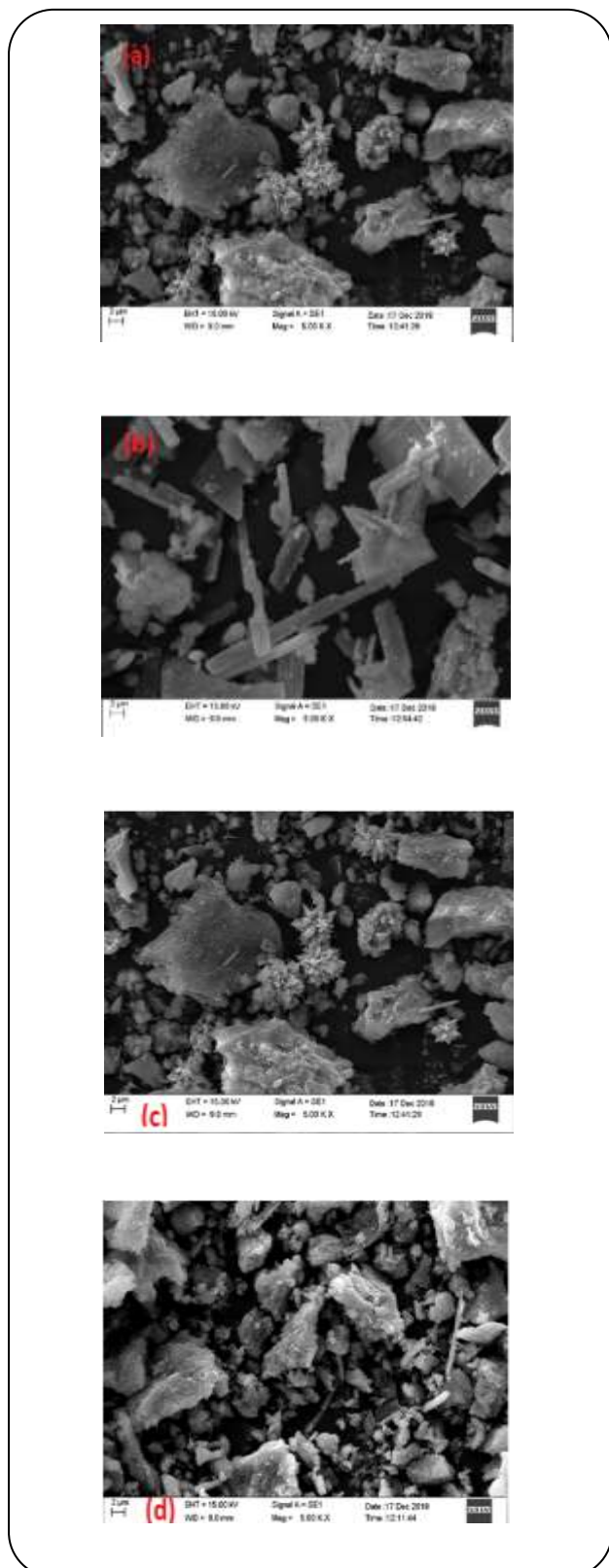


Fig. 8: SEM image of the catalyst prepared using (a) hydrothermal method (b) co-precipitation method (c) sol-gel method (d) wet impregnation method.

the main parameter that affects the adsorption process because of its impact on the surface charge of the photocatalyst. In this study, the result of pH was examined for the decolorization of 100 PPM dye solution by varying pH from 3 to 9 under a constant photocatalyst dose 0.5 g/L and 125W UV-lamp irradiation. The results indicate that the photo-decolorization increases with an increase in pH of the solution from 7 to 9, as shown in Fig. 10. This may be attributed to the behavior of the Zn-based photocatalyst, also at higher pH deprotonation occurs for the surface hydroxy of bone char which results in a negative charge on the catalyst surface [8]. The surface of Zn/BC composite is positively charged at lower pH while it becomes negatively charged at higher pH. As brilliant green is a cationic dye, the higher pH values help to get more decolorization efficiency [26, 27]. Also, in the alkaline phase, a large amount of hydroxyl (OH^-) ions is oxidized with the positively charged holes (h^+) to produce hydroxyl (HO^\bullet) radicals [4]. But the stability of Zn/BC composite at higher pH values might not be ensured because of the alkaline dissolution of ZnO [26].

Jia *et al.* (2018) reported the synthesis of ZnO/BC composite (photocatalyst), its characterization, and its application for the removal of methylene blue dye from wastewater effluent [8]. They have studied the photocatalytic activity of this novel composite for the different experimental parameters, including the effect of oxygen, pH, positively charges holes, and hydroxyl radicals. From the obtained results, it was clear that the dissolved oxygen contributes to the photocatalysis process for the removal of methylene blue dye in alkaline conditions. As discussed previously, the photocatalytic processes strongly depend on the pH of the solution. The increase in the dye concentration on bone-char (BC) increases the contact of positively charged holes (h^+) and hydroxyl (OH^\bullet) radicals generated on the catalyst surface. This fact enhances the whole photocatalytic process for the removal of respective water pollutants. Jia *et al.* (2018) obtained the dye removal efficiency of 80-90%, which closely matches the removal efficiency of BG dye, 87.8% (our study). Rangkooy *et al.* (2013) studied the photocatalytic remediation of formaldehyde using ZnO-BC composite. They found the removal efficiency between 40-73% for the initial concentration range of 2.5 to 25 mg/m^3 [9]. It was found that the strong adsorption of the formaldehyde molecules on bone-char, results in a higher rate of diffusion onto the photocatalyst surface. Furthermore,

enhances the photocatalysis process. In our study, the optimum dye removal efficiency was found to be 87.8% for the initial concentration of 100 ppm and with the photocatalyst dose of 0.5 g/L.

Effect of photocatalyst dosage on the percentage decolorization

In the photocatalysis process, the dosage of the photocatalyst plays an active role as it is directly proportional to the overall rate of catalysis [28]. The degradation of 100 ppm BG solution was carried out by varying the photocatalyst dose from 0.1-1 g/L under 125 W UV-lamp at pH 9. Fig. 11 represents the influence of catalyst dosage on the decolorization efficiency of brilliant green dye. The decolorization efficiency was found to increase with an increase in catalyst dose from 0.1 to 0.5 g/L due to the photogeneration of more electron-hole pairs, which further produce free radicals and help to degrade more BG dye concentrations. The increase in the concentration of photocatalyst dosage (from 0.1 to 0.5 g/L), shows an increase in the decolorization of BG dye. This is due to the fact that the number of dye molecules got adsorbed and thus, the photons were adsorbed. The photons adsorbed enhanced with an increase in photocatalyst loading [29]. The increase in dye decolorization was probably due to an increase in the availability of catalytic sites and adsorption sites. But, also increasing the photocatalyst dosage beyond the optimum, the decolorization rate declined. This might have happened due to the excess catalyst could damage the transparency of the solution, resulting in a light scattering effect and reducing the penetration of light through the BG solution. Hence, the photocatalytic activity decreases [17,30]. Moreover, the increase in the catalytic loading beyond 0.5 g/L may result in the agglomeration of photocatalyst particles. Thus, the part of the photocatalyst surface becomes unavailable for photon absorption, and the decolorization rate of BG dye decreases.

KINETIC STUDY

The kinetics of photocatalytic decolorization of different organic pollutants has been described with Langmuir-Hinshelwood (LH) model. This model (Eq.(7)) determines the relationship between initial dye concentration and photodegradation rate.

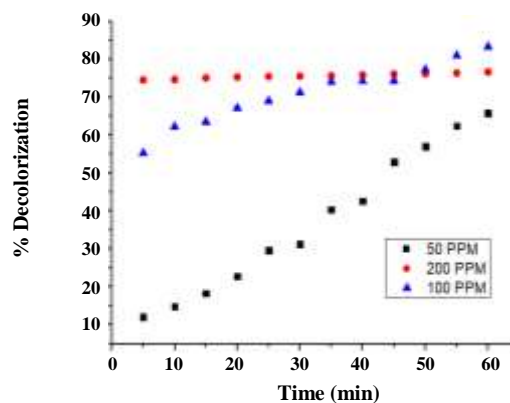


Fig. 9: Effect of initial dye concentration on its percentage decolorization in UV-photolysis (125W UV-lamp irradiation).

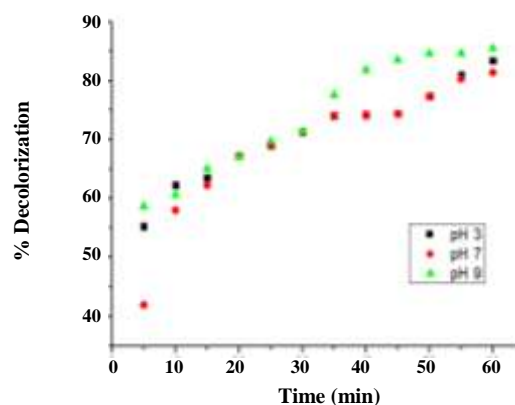


Fig. 10: Effect of pH on decolorization efficiency of brilliant green dye. (Reaction conditions: BG concentration: 100 g/L, ZnO/BC catalyst dose: 0.5 g/L, 125W UV-lamp irradiation).

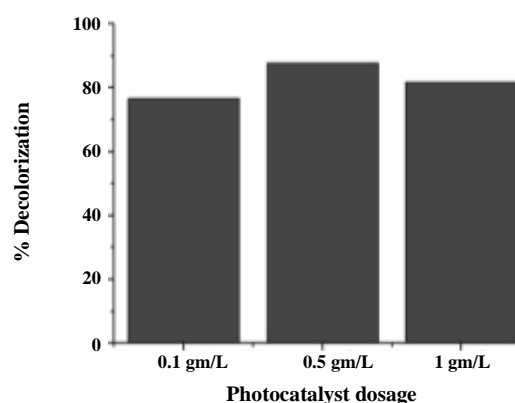


Fig. 11: Effect of photocatalyst dose on the decolorization efficiency of brilliant green dye. (Reaction conditions: BG concentration: 100 ppm, pH 9, 125W UV-lamp irradiation).

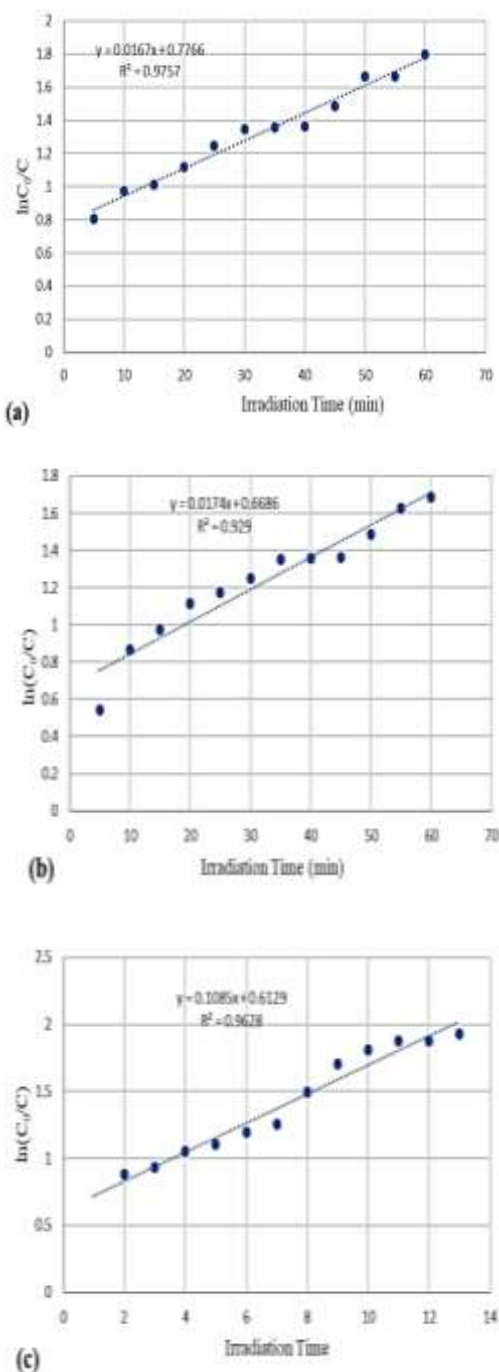


Fig. 12: Pseudo-first order kinetics for Brilliant green dye in the presence of photocatalyst ZnO/BC catalyst at (a) pH 3, (b) pH 7, (c) pH 9.

$$\frac{1}{k_{\text{obs}}} = \frac{1}{k_{\text{LH}} K_c} + \frac{BG}{k_c} \quad (7)$$

Where *BG*, initial dye concentration in mg/L, k_{LH} , Langmuir-Hinshelwood adsorption equilibrium constant

(L/mg), and k_c = rate constant (in mg/L/min). Experimental results showed the photocatalytic decolorization of BG dye with ZnO/BC photocatalyst follows pseudo-first-order kinetics. At a lower initial dye concentration, the rate expression is represented as per Eq. (8).

$$r = - \frac{d[BG]}{dt} = k_{\text{app}} [BG] \quad (8)$$

The integration of this equation will lead to the relation with restriction $C=C_0$ at $t=0$ with C_0 being the equilibrium concentration of the bulk solution. The kinetic study of ZnO/BC composite for BG dye decolorization was studied with Langmuir-Hinshelwood kinetic model and expressed in terms of Eq. (9) [31].

$$\ln \frac{C_0}{C} = k_{\text{app}} t \quad (9)$$

Where, k_{app} is the pseudo-first-order rate constant and C_0 is the initial concentration of BG dye and C is the concentration of BG dye after irradiation time, t .

A plot of $\ln(C_0/C)$ versus photo-irradiation time (t) for BG dye decolorization at different solution pH values is represented in Fig. 12. A linear relation was observed between the decolorization of BG dye and irradiation time, so each sample follows first-order reaction kinetics. The slope of the line passing through the origin gives the rate constant k for the photodegradation of BG dye. Table 3 represents the values for rate constant, half-life time, linear regression coefficient (R) and R^2 obtained.

CONCLUSIONS

In summary, the Zn/Bone-Char photocatalyst was successfully synthesized via four different methods, i.e., wet impregnation, hydrothermal, precipitation, and sol-gel methods. The bone char prepared from chicken bone was used as a carbon-based material making this catalyst economical as well as eco-friendly. The synthesized photocatalysts were characterized by XRD, FT-IR, BET, and SEM techniques to analyze the physicochemical properties. The catalyst prepared by the sol-gel method has a large specific surface area 61.034 m²/g and it was applied for the treatment of BG dye solution. The catalyst showed prominent photocatalytic activity and successfully decolorized 87.8% of BG dye solution with 100 mg/L concentration under 125 W UV-lamp irradiation within 60 min. So, it can be concluded that bone char increases

Table 3: Kinetic data for photodegradation of brilliant green dye by ZnO/BC catalyst at different pH values.

Sample	Rate Constant (min) ⁻¹	t _{1/2} (min)	R	R ²
pH 3	0.0167	41.50	0.9877	0.9757
pH 7	0.0174	39.83	0.9638	0.929
pH 9	0.1085	6.38	0.9812	0.9628

the visible light activity of the semiconductors and makes them more suitable for the treatment of industrial effluents. Finally, it can be concluded that the photocatalysis of BG dye by using ZnO/BC photocatalyst follows pseudo-first-order kinetics.

Received : Oct. 10, 2020 ; Accepted : May 3, 2021

REFERENCES

- [1] Pereira L.A., Couto A.B., Almeida D.A.L., Ferreira N.G., Singular Properties of Boron-Doped Diamond/Carbon Fiber Composite as Anode in Brilliant Green Dye Electrochemical Degradation, *Diam. Relat. Mater.*, **103**: 107708 (2020).
- [2] El Nemr A., Hassaan M.A., Madkour F. F., Advanced Oxidation Process (AOP) for Detoxification of Acid Red 17 Dye Solution and Degradation Mechanism, *Environ.Process.*, **5**: 95-113 (2018).
- [3] Jia P., Tan H., Liu K., Gao W., Enhanced Photocatalytic Performance of ZnO/Bone Char Composites, *Mater. Lett.*, **205**: 233-235 (2017).
- [4] Jia P., Tan H., Liu K., Gao W., Synthesis, Characterization and Photocatalytic Property of Novel ZnO/Bone Char Composite, *Mater. Res. Bull.*, **102**: 45-50 (2018).
- [5] Nguyen C.H., Tran M.L., Van Tran T.T., Juang R.S., Enhanced Removal of Various Dyes from Aqueous Solutions by UV and Simulated Solar Photocatalysis over TiO₂/ZnO/rGO Composites, *Sep. Purif. Technol.*, **232**:115962 (2020).
- [6] Kumar A., Sharma G., Naushad M., Garcia-Penas A., Mola G.T., Si C., Stadler F.J., Bio-Inspired and Biomaterials-Based Hybrid Photocatalysts for Environmental Detoxification: A Review, *Chem. Eng. J.*, **382**: 122937 (2020).
- [7] Gholami P., Khataee A., Soltani R. D. C., Dinpazhoh L., Bhatnagar A., Photocatalytic Degradation of Gemifloxacin Antibiotic Using Zn-Co-LDH@biochar Nanocomposite, *J. Hazard. Mater.*, **382**: 121070 (2020).
- [8] Jia P., Tan H., Liu K., Gao W., Synthesis and Photocatalytic Performance of ZnO/Bone Char Composite, *Materials.*, **11**: 1981 (2018).
- [9] Rangkooy H.A., Rezaee A., Khavanin A., Jonidi Jafari A., Khoopaie A.R., A Study on Photocatalytic Removal of Formaldehyde from Air Using ZnONanoparticles Immobilized on Bone Char, *Qom Univ. Med. Sci. J.*, **7**: 17-26 (2013).
- [10] Gole V.L., Gogate P.R., Degradation of Brilliant Green Dye Using Combined Treatment Strategies Based on Different Irradiations, *Sep. Purif. Technol.*, **133**: 212-220 (2014).
- [11] Kismir Y., Aroguz A.Z., Adsorption Characteristics of the Hazardous Dye Brilliant Green on SaklıkentMud, *Chem. Eng. J.*, **172**: 199-206 (2011).
- [12] Yu J., Jiang C., Guan Q., Ning P., Gu J., Chen Q., Zhang J., Miao R., Enhanced Removal of Cr (VI) from aqueous Solution by Supported ZnO Nanoparticles on Biochar Derived from WasteWater Hyacinth, *Chemosphere.*, **195**: 632-640 (2018).
- [13] Liu S., Sun H., Suvorova A., Wang S., One-Pot Hydrothermal Synthesis of ZnO-Reduced Graphene Oxide Composites Using Zn Powders for Enhanced Photocatalysis, *Chem. Eng. J.*, **229**:533-539 (2013).
- [14] Chanu L.A., Singh W.J., Singh K.J., Devi K.N., Effect of Operational Parameters on the Photocatalytic Degradation of Methylene Blue Dye Solution Using Manganese Doped ZnO nanoparticles, *Results Phys.*, **12**: 1230-1237 (2019).
- [15] Rezaee A., Rangkooy H., Khavanin A., Jafari A.J., High Photocatalytic Decomposition of the Air Pollutant Formaldehyde Using Nano-ZnO on Bone Char, *Environ. Chem. Lett.*, **12**:353-357 (2014).
- [16] Hadjltaief H.B., Ameer S.B., Da Costa P., Zina M. B., Galvez M.E., Photocatalytic Decolorization of Cationic and Anionic Dyes over ZnO Nanoparticle Immobilized on Natural Tunisian Clay, *Appl. Clay Sci.*, **152**: 148-157 (2018).

- [17] Li S.Q., Zhou P.J., Zhang W.S., Chen S., Peng H., Effective Photocatalytic Decolorization of Methylene Blue Utilizing ZnO/rectorite Nanocomposite under Simulated Solar Irradiation, *J. Alloys Compd.*, **616**: 227-234 (2014).
- [18] Souza S.P.M.C., Araujo E.G., Morais F.E., Santos E.V., Silva M.L., Martinez-Huitle C.A., Fernandes N.S., Determination of Calcium in Tablets Containing Calcium Citrate Using Thermogravimetry (TG), *Braz. J. Therm. Anal.*, **2**: 17-22 (2013).
- [19] Runyut D.A., Robert S., Ismail I., Ahmadi R., Abdul Samat N.A.S.B., Microstructure and Mechanical Characterization of Alkali-Activated Palm Oil Fuel Ash, *J. Mater. Civil Eng.*, **30**: 04018119 (2018).
- [20] Wei W., Yang L., Zhong W. H., Li S. Y., Cui J., Wei Z.G., Fast Removal of Methylene Blue from Aqueous Solution by Adsorption onto Poorly Crystalline Hydroxyapatite Nanoparticles, *Dig. J. Nanomater. Biostruct.*, **19**: 1343-1363 (2015).
- [21] Smolen D., Chudoba T., Malka I., Kedzierska A., Lojkowski W., Swieszkowski W., Kurzydowski K. J., Lewandowska Szumiel M., Highly Biocompatible, Nanocrystalline Hydroxyapatite Synthesized in a Solvothermal Process Driven by High Energy Density Microwave Radiation, *Int. J. Nanomedicine*, **8**: 653 (2013).
- [22] Fatimah I., Yudha S.P., Sopian K.D., Ratnasari D.L., Effect of Zn Content on the Physicochemical Characteristics and Photoactivity of ZnO Supported Activated Carbon, *Orient. J. Chem.*, **32**: 2757-2768 (2016).
- [23] Moreira A.J., Borges A.C., Gouveia L.F.C., Macleod T.C.O., Freschi G.P.G., The Process of Atrazine Degradation, Its Mechanism, and the Formation of Metabolites Using UV and UV/MW Photolysis, *J. Photochem. Photobiol. A*, **347**: 160-167 (2017).
- [24] Mahmoud, M.S., Decolorization of Certain Reactive Dye from Aqueous Solution Using Baker's Yeast (*Saccharomyces cerevisiae*) Strain, *HBRC J.*, **12**: 88-98 (2016).
- [25] Abdellah M.H., Nosier S.A., El-Shazly A.H. Mubarak A.A., Photocatalytic Decolorization of Methylene Blue Using TiO₂/UV System Enhanced by Air Sparging, *Alex. Eng. J.*, **57**: 3727-3735 (2018).
- [26] Li S.Q., Zhou P.J., Zhang W.S., Chen S., Peng H., Effective Photocatalytic Decolorization of Methylene Blue Utilizing ZnO/rectorite Nanocomposite under Simulated Solar Irradiation, *J. Alloys Compd.*, **616**: 227-234 (2014).
- [27] Jiang Y., Sun Y., Liu H., Zhu F., Yin H., Solar Photocatalytic Decolorization of CI Basic Blue 41 in an Aqueous Suspension of TiO₂-ZnO, *Dyes Pig.*, **78**: 77-83 (2008).
- [28] Eydivand S., Nikazar M., Degradation of 1,2-Dichloroethane in Simulated Wastewater Solution: A Comprehensive Study by Photocatalysis Using TiO₂ and ZnO Nanoparticles, *Chem. Eng. Commun.*, **202**: 102-111 (2015).
- [29] Munusamy S., Aparna R., Prasad R., Photocatalytic Effect of TiO₂ and the Effect of Dopants on Degradation of Brilliant Green, *Sustain. Chem. Process*, **1**: 1-8 (2013).
- [30] Zhu C., Wang L., Kong L., Yang X., Wang L., Zheng S., Chen F., Mai Zhi F., Zong H., Photocatalytic Degradation of Azo Dyes by Supported TiO₂+UV in Aqueous Solution, *Chemosphere*, **41**: 303-309 (2000).
- [31] Bhatia S., Verma N., Photocatalytic Activity of ZnO Nanoparticles with Optimization of Defects, *Mater. Res. Bull.*, **95**: 468-476 (2017).